ACS OMEGA

ACS AUTHORCHOICE

http://pubs.acs.org/journal/acsodf

Article

Desulfurization Characteristics of Fuel-Born Alkali and Alkali Earth Metal Compounds in Coal Ashes from Lab-Scale Experiment to Real-Scale Monitoring of CFBC and PC Boiler

Dong-Yeop Kim, In-Duck Cheong, Jeonggeon Kim, and Donggeun Lee*

Cite This: *ACS Omega* 2021, 6, 5962−5971

Read Online

ACCESS | Metrics & More | Article Recommendations

ABSTRACT: Previous research findings and experiential accounts have provided evidence that specific components of coal ash play a catalytic role in the dry desulfurization of flue gas such that their contributions need to be considered for determining the optimal amount of desulfurizing agent such as limestone. The purpose of this study was to quantify the desulfurization characteristics of coal ash in a 500 MW pulverized coal combustion (PC) boiler as well as a 1000 MW circulating fluidized bed combustion (CFBC) boiler. In parallel with a year-long data collection of coal blends and emission characteristics, a series of temperature-controlled fixed bed (lab scale) experiments were conducted for 11 individual (but representative) coal samples. The results indicated that desulfurization by fly ashes appeared to proceed roughly in proportion to the total alkali (TA) contents of the ash, which were consistent with our preliminary test result of the CFBC boiler. In the PC boiler, however, the desulfurization reaction seemed to be very kinetically limited, apparently deactivating the TA components. We developed a practical equation for a priori prediction of SO_2 concentration based on the sulfur content of coal blends.

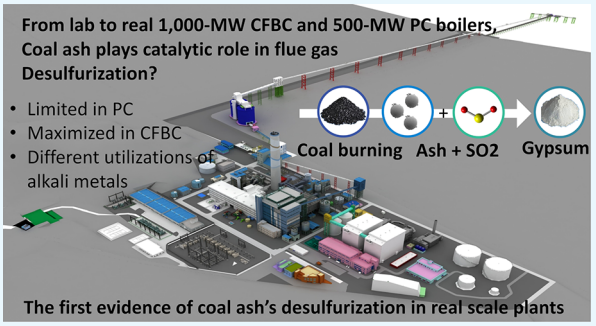

1. INTRODUCTION

Unlike gaseous nitrogen oxide (NO_x), sulfur oxides (SO_x), mostly in the form of SO_2, are produced directly from fuel itself during its combustion in power plants and are emitted into the air.[1,2] Since gaseous SO_2 is a primary air pollutant as well as a major precursor of atmospheric PM2.5 dusts, many sources utilizing solid fuels with high levels of sulfur, such as coal-fired power plants, are being monitored for their SO_2 emissions. The concentration of SO_2 in flue gas (C_{SO2}) is readily estimated by eq 1 based on ultimate analysis results of coals.

$$C_{SO2}(\mathrm{mL/Nm^3}) = \frac{\frac{22.4}{32} \times S}{G_w} \times 10^4 \quad (1)$$

where S denotes the sulfur contents (wt %) of coals (as-fired basis, hereafter AFB) and G_w is defined as the flow rate of wet flue gas per 1 kg of coal (Nm^3/kg·coal).

Boiler engineers have learned through extensive field experience that the actual concentration of SO_2 at the inlet of a flue gas desulfurization (FGD) unit is always lower than the theoretical fuel-born SO_2 concentration calculated by eq 1. In reality, a smaller amount of desulfurization agents may be consumed in wet FGD units of pulverized coal combustion (PC) boilers compared with the theoretical requirement per sulfur content of fuels. In circulating fluidized bed combustion (CFBC) boilers, one case was reported in which combustion failure occurred when desulfurizing agents such as lime were added up to the design level without consideration of the catalytic effect of ash components on desulfurization.[3] It is therefore of particular interest to optimize the amount of desulfurizing adsorbent with reference to the content of fuel-born catalysts in ash.[4,5]

To date, no solid consensus has been reached on how to determine the optimal amount of adsorbents or how to quantitatively assess the catalytic effects of ash components under real-world circumstances.[6] This is the main reason for the delay from plant construction to operational optimization. According to a pilot-scale PC boiler study,[7] SO_2 concentration is reduced mainly by heterogeneous condensation onto alkali-rich fly ash particles, and SO_2 removal is dominated by sodium regardless of the calcium content in ash. Elsewhere, a real-scale study of a PC boiler[8] reported that the intrinsic desulfurization effect of ash was enhanced in linear proportion to the content of

Received: January 14, 2021
Accepted: February 8, 2021
Published: February 15, 2021

https://dx.doi.org/10.1021/acsomega.1c00177
ACS Omega 2021, 6, 5962−5971

free active CaO in ash. Although these two works are notable as being the first large-scale studies, the results appear dubious in view of the catalytic effect of calcium. The results are also inconsistent with other studies[1,2,9−11] on identifying the most significant ash component for desulfurization and the underlying mechanism.

Cheng et al.[12] provided a comparative review of alkaline compounds in coal ash, limestone, and other oxides, in their desulfurization efficiencies in PC boilers and several lab-scale furnaces, and noted that the desulfurization efficiency of solid adsorbents can be greatly affected by the thermal stability of the resulting sulfates. Even 10 years later, Mathieu et al.[13] are still listing desulfurization capacities of various solid sorbents ranging from single oxide to mixed oxide, oxides on carbons, and oxides on porous silica and talking about their advantages and drawbacks mostly on the basis of lab-scale and pilot-scale facilities under precise control of coal types and operation conditions. They also focused on what happens microscopically in solid sorbents. More recently, Spörl et al.[10] conducted experiments for SO_2-to-SO_3 conversion by ash under various oxy-firing conditions in a pilot-scale furnace, summarizing that higher ash contents are beneficial for capturing SO_3 on a baghouse filter, while other alkaline species such as Mg, K, and Na in ash, not Ca alone, play a role in the SO_3 capture. Belo et al.[1,11] investigated the catalytic effects of fly ash on SO_2-to-SO_3 conversion under air- and oxy-firing conditions in a lab-scale tubular furnace and reconfirmed the catalytic function of iron oxide in ash for SO_3 formation. Most recently, Wang et al.[14] returned to a fundamental study on sulfation reaction routes of limestone with emphasis on surface porosity change of limestone particles. Li et al.[15] performed a similar work with limestone using pilot-scale reactors under air-firing/oxy-firing fluidized bed conditions and reported a near-complete sulfation of limestone in 60 min at 850 °C under air firing.

The aforementioned technological progress is obviously helpful to broaden our perspectives on the desulfurizing effect of various alkali and alkali earth metal (AAEM) species in coal ashes. However, it should be noted that most of the previous studies on the effects of AAEM species have been made on the basis of lab-scale or pilot-scale reactors. This implies that it is still questionable to directly apply the results to the real boiler systems that undergo large variations in coal types, sulfur contents, and ash contents and compositions[12,13] on a daily basis. Another challenge can be created by the blending of two or three coals of different reactivity, as widely undertaken by current power stations. Although coal blending is effective in providing a consistent feedstock of fuel with a predictable calorific value of the blend, it can also cause the properties of coal blends to vary considerably every day. As such, these complexities force boiler engineers to be conservative in consideration of dry desulfurization in PC boilers or optimal addition of desulfurization agents in CFBC boilers. In fact, the current FGD units installed in power plants are dominated by wet-scrubbing technology,[16] and there is no report available on a complete data set that includes the entire properties of coal as well as flue gas compositions in a real-scale power plant.

Thus, this study was designed to fill the gap between the real-scale boilers and lab-scale studies through a boiler engineer's eye. Those engineers in power plants are not interested in coal ash itself unless the quality of gypsum product is of interest[16] but rather need some sorts of practical guidance for the stable and economic operation of their boilers with an optimal (minimal) dose of limestone. To fulfill the need, we attempted to establish a database (DB) of the complete field data recorded across 1 year in a 500 MW PC boiler in Korea. Second, the year-long collection of field data was statistically analyzed to find a practically reliable correlation between the blended coal properties and SO_2 emissions. In parallel with the field study, a series of fixed bed desulfurization experiments under temperature control were conducted for 11 pulverized coal samples that have most widely been used in the same boiler. Transient desulfurization behaviors of ash components per coal type were identified, relating the coal and ash properties to SO_2 concentration in time. The results indicated that the desulfurization of fuel-born catalysts in ash is kinetically limited in a PC boiler but seemingly strengthened in a CFBC boiler. Lastly, a practical equation was developed for a priori prediction of SO_2 concentration based on the composition of coal blends.

2. THEORY

As seen in eq 2, dry desulfurization is described by a heterogeneous sulfation reaction of gaseous SO_2 on the surface of solid metal oxide particles.[12,13]

$$\mathrm{MeO} + \mathrm{SO_2} + \frac{1}{2}\mathrm{O_2} \leftrightarrow \mathrm{MeSO_4} \tag{2}$$

where Me represents alkali or alkaline earth metal elements of desulfurization agents, such as Ca in limestone. One may notice that the role of the Me (AAEM species) in eq 2 is not the same as conventional catalysts that generally react with reactants to form intermediates and subsequently produce the final reaction product in the process regenerating the catalyst. Rather, AAEM species seem to participate in the reaction more likely as additional reactants with no further regeneration step. AAEM species, if existing in addition to CaO in ash, could provide additional pathways for sulfur capture, which results in an acceleration of the sulfation reaction similar to catalysts. Thus, those species were mentioned as if they were catalysts to highlight the apparent effect.

Dry desulfurization of limestone is known to occur through either an indirect or a direct sulfation path, depending on the gas temperature and CO_2 concentration in flue gas.[15−17] When the temperature is as low as 800−950 °C or CO_2 concentration is high like under oxy-firing condition in CFBC boilers, limestone undergoes a direct sulfation reaction ($CaCO_3 + SO_2 + {}^1/_2O_2 \rightarrow CaSO_4 + CO_2$). In contrast, in air-firing PC boilers where the temperature is as high as 1200−1500 °C and CO_2 level is low, limestone is first decomposed into CaO by calcination reaction ($CaCO_3 \rightarrow CaO + CO_2$) and then reacted with SO_2 by sulfation reaction of lime ($CaO + SO_2 + {}^1/_2O_2 \rightarrow CaSO_4$).

It is the molar elemental ratio of calcium to sulfur (simply called Ca/S ratio and defined as R in eq 3) that determines the efficiency of dry desulfurization. As for limestone, theoretically 1 mol of Ca is needed for removing 1 mol of SO_2, which represents the stoichiometric (or theoretical) ratio of Ca/S being unity.[10,13,17−19] In reality, despite the excellent SO_2-capture capability of limestone, high levels of excess limestone injection such as Ca/S ≥ 3 are often employed to achieve desulfurization efficiency of greater than 90%.[20,21] In general, such a Ca/S molar ratio is predetermined at the boiler design stage with respect to the boiler specifications, its operation condition, and coals' characteristics.

$$R = \frac{\mathrm{Ca}}{\mathrm{SO_{2,in}}} = E_{\mathrm{sor}}\frac{\mathrm{Ca}}{\mathrm{SO_{2,in}} - \mathrm{SO_{2,out}}} \tag{3}$$

https://dx.doi.org/10.1021/acsomega.1c00177
ACS Omega 2021, 6, 5962−5971

Table 1. Sulfur and Ash Contents of 11 Representative Coals and Their Ash Compositional Analysis Data

			ash ingredients (%, DB)								
coal name (country[a])	S (%, ARB)	ash (%, ADB)	SiO_2	Al_2O_3	Fe_2O_3	CaO	MgO	Na_2O	K_2O	SO_3	etc
Adaro (IDN)	0.13	4.41	32.86	11.21	16.42	15.05	14.33	0.56	0.65	8.03	0.89
Kideco (IDN)	0.11	5.20	29.37	11.17	28.56	13.97	7.20	0.40	0.62	7.92	0.79
Indominco (IDN)	1.37	9.05	51.12	25.71	10.42	4.09	3.01	1.61	2.14	0.07	1.83
Flame (AUS)	0.64	21.36	69.78	18.81	5.73	1.18	0.42	0.39	0.81	1.33	1.55
Moolarben (AUS)	0.44	17.29	81.04	16.26	1.13	0	0	0.29	0.44	0.03	0.81
Trafigura (AUS)	0.80	18.42	62.95	24.60	7.64	0.62	0.58	0.44	1.68	0.09	1.40
Anglo (ZAF)	0.50	13.97	48.29	29.59	4.14	7.80	1.80	0.31	0.59	3.32	4.16
Mercuria (ZAF)	0.58	17.41	51.68	28.96	5.63	5.40	1.09	0.36	0.69	3.08	3.11
Macquarie (COL)	0.67	8.46	55.46	19.48	9.97	3.42	1.59	2.71	2.09	3.94	1.34
Cloudpeak (CAN)	0.51	5.74	38.62	21.43	6.42	15.54	4.46	4.74	1.09	6.08	1.62
Tugnuisky (RUS)	0.44	10.66	59.40	22.48	8.57	2.62	1.74	1.68	2.14	0.14	1.23

Note: ARB, as-received basis; ADB, air-dried basis; and DB, dry basis. [a]Country name was denoted in accordance with ISO 3166 three-letter country codes.

where Ca is the amount of calcium (in units of mol/kg·coal) in the added adsorbent (limestone), $SO_{2,in}$ is the amount of sulfur in the coal used (in units of mol/kg·coal), $SO_{2,out}$ is the amount of sulfur remaining in the flue gas after desulfurization (in units of mol/kg·coal), and E_{sor} is the desulfurization efficiency as defined by $(SO_{2,in} - SO_{2,out})/SO_{2,in}$.

Once the ratio R is determined, it is straightforward to calculate the feed rate of limestone. For instance, when CaO content in coal ash is negligible, the required feed rate of limestone L_q per unit mass of coal is calculated by eq 4.[5]

$$L_q = \frac{100S}{32X_{CaCO3}}R \tag{4}$$

where S is the mass fraction of sulfur in coal (wt %), X_{CaCO3} is the purity of limestone defined by the mass fraction of $CaCO_3$ in the limestone, R is the ratio defined in eq 3, and the numbers 100 and 32 represent the molar mass (kg/kmol) of $CaCO_3$ and sulfur, respectively.

Considering the problems arising from the excessive use of limestone, the optimal feed rate of limestone may be estimated by precluding the intrinsic removal of SO_2 by the fuel-born catalysts,[5] such as eq 5.

$$L_q' = \frac{100S}{32X_{CaCO3}}(R - R') \tag{5}$$

where L_q' is the corresponding feed rate of limestone per unit mass of the coal in units of (ton·adsorbent/ton·coal) and R' is the intrinsic Ca/S molar ratio associated with the relative amount of fuel-born CaO species. Given the mass fraction of CaO per unit mass of coal (X_{Ca}), eq 6 shows how to calculate R'.[5]

$$R' = \frac{32X_{Ca}}{56S} \tag{6}$$

Meanwhile, eqs 5 and 6 are not used in real CFBC boiler operation, but rather, the feed rate is usually adjusted based on field experience for maintaining the SO_2 emission level below the legislative emission limit.[4−6] Another point to note is that eqs 5 and 6 were derived on the only basis of the Ca content in ash. This might be debatable because other alkali and alkali earth metal oxides are also known to exhibit catalytic desulfurization functions to some degree.[10] For instance, MgO was reported to play some role of catalysts but also proposed to prevent the sintering of CaO (by dispersing CaO crystals) particularly in PC boilers.[12,13] In the presence of SiO_2 and CaO, Fe_2O_3 was reported to improve the thermal stability of $CaSO_4$ probably through the Fe−Si−Ca system in PC boilers.[12] As such, coal ashes are essentially mixed oxides so that their components can interact with each other to create an additional synergetic effect. This makes the impact analysis per individual AAEM species further complicated and questionable. This is why we treated the total alkaline metal (TA) species in ash as a whole[9] even though it is less precise.

Under the assumption that the TA is a single inherent desulfurization agent, eqs 5 and 6 are modified into eqs 7 and 8 by replacing X_{Ca} with the mass fraction of TA per unit mass of coal (X_{TA}). In the new equations, $R^{"}$ is the inherent TA/S molar ratio similar to R', and $L_q^{"}$ is the modified feed rate of limestone per unit mass of coal.[5] In eq 7, the number 56 implies that the TA will be treated as the CaO equivalent.

$$R^{"} = \frac{32X_{TA}}{56S} \tag{7}$$

$$L_q^{"} = \frac{100S}{32X_{CaCO3}}(R - R^{"}) \tag{8}$$

Using eq 5 or 7 enables one to relate the measured SO_2 concentration with Ca or TA contents in coal ash, respectively, from which the desulfurization potential of each species is identified by comparison.

3. EXPERIMENTAL SECTION

3.1. Sample Preparation and Characterization. Eleven types of coals, taking into account their production countries, were selected as representative coals among the bituminous and sub-bituminous coals that had been used for 1 year in a domestic coal-fired power plant. A commercial limestone being used was also considered as a reference sample. An ash sample for each coal was prepared in accordance with the standard test method of major and minor elements in coal (ASTM D 4326-13) except that the coal-burning temperature was 850 °C, higher than the ASTM suggestion (750 °C) for shortening the time. All ash samples were equally ball-milled and made to a similar size (10−50 μm), and the limestone was milled to a diameter of 500−600 μm, which is similar to the size used in a real power plant.

The total moisture on an as-received basis (ARB), proximate analysis data on an air-dried basis (ADB), and ultimate analysis data on a dry basis (DB) of the selected coal samples were determined directly from Korea's Hadong Thermal Power Plant.

https://dx.doi.org/10.1021/acsomega.1c00177
ACS Omega 2021, 6, 5962−5971

Table 2. Estimation of Theoretical (Maximum) Adsorption per Sample Mass Based on CaO and TA Contents of the 11 Representative Coal Ashes and the Comparison with Its Corresponding Saturated Adsorption Capacity (mg·SO_2/g·Adsorbent) from the Fixed Bed Experiment

	alkali & alkali earth (mol/100 g·sample)		theoretical adsorption (mg·SO_2/g·sample)		experimental result (mg·SO_2/g·sample)		maximum utilization (%)	
coal name	CaO	TA	by CaO	by TA	saturated	2 min cut	by CaO	by TA
Adaro[a]	0.268	**0.640**	171.9	**409.9**	**223.31**	**13.29**	**129.9**	**54.5**
Kideco[a]	0.249	**0.441**	159.6	**282.4**	**145.50**	**13.65**	**91.2**	**51.5**
Indominco[b]	0.073	0.196	46.7	125.8	5.02	3.71	10.7	4.0
Flame[b]	0.021	0.046	13.5	29.7	5.09	3.48	37.8	17.1
Moolarben[b]	0.000	0.009	0.0	6.0	1.87	1.47	0	31.2
Trafigura[b]	0.011	0.050	7.1	32.3	1.66	1.56	23.4	5.1
Anglo[a]	0.139	**0.195**	89.1	**124.9**	**13.92**	**6.43**	**15.6**	**11.1**
Mercuria[b]	0.096	0.136	61.7	87.4	1.95	1.71	3.2	2.2
Macquarie[b]	0.061	0.166	39.1	106.6	3.83	3.54	9.8	3.6
Cloud Peak[a]	0.277	**0.476**	177.5	**304.8**	**72.49**	**10.48**	**40.8**	**23.8**
Tugnuisky[b]	0.047	0.140	29.9	89.5	4.75	3.66	15.9	5.3
Limestone[a,*]	0.954	**0.985**	611.0	**631.0**	**127.85**	**15.28**	**20.9**	**20.3**

[a]Group A: coal ash samples and limestone* that took long to reach the saturation of desulfurization and highlighted in bold. [b]Group B: coal ash samples that were quickly saturated, denoting low saturation adsorption capacity.

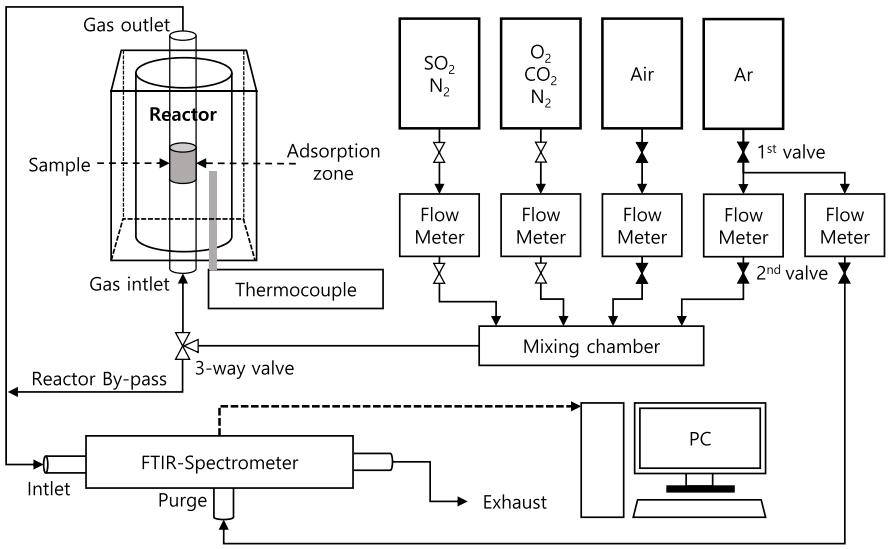

Figure 1. Schematic diagram of the experimental setup for fixed bed adsorption experiments.

The sulfur and ash contents of the coals were additionally measured in accordance with ASTM D 4239-17 and 7582-15, respectively. X-ray fluorescence spectroscopy (XRF) was also used for composition analysis of the ash samples, and the results are listed in Table 1. For convenience of analysis, the mole content (Y_{TA}) of total alkali and alkali earth metal compounds (TA) is expressed as the total mole numbers of TA in 100 g of ash by eq 9, and the results are summarized in Table 2. The Y_{TA} is simply converted to the mass unit (X_{TA}) but as the CaO equivalent by eq 10.[9,10]

$$Y_{TA}(\text{mol}/100\ \text{g·ash}) = \frac{\text{g CaO}/100\ \text{g}}{56.10\ \text{g/mol}} + \frac{\text{g Na}_2\text{O}/100\ \text{g}}{61.98\ \text{g/mol}} + \frac{\text{g MgO}/100\ \text{g}}{40.31\ \text{g/mol}} + \frac{\text{g K}_2\text{O}/100\ \text{g}}{94.20\ \text{g/mol}} \quad (9)$$

$$X_{TA}(\text{g}/100\ \text{g·ash}) = Y_{TA}(\text{mol}/100\ \text{g·ash})\cdot 56(\text{g/mol·CaO}) \quad (10)$$

3.2. Temperature-Controlled Fixed Bed Adsorption Experiment. Figure 1 illustrates the experimental setup for the fixed bed adsorption characterization of the as-prepared ash samples. A test section holding 0.5 g of ash sample with glass fiber filters was fitted into a quartz tube with an inner diameter of 33.7 mm, and the assembly was positioned in the middle of a tube furnace. While heating the furnace, Ar gas was fed at a rate of 1.25 L/min (corresponding to a space velocity of 37,783 h^{-1}) for flushing the entire gas lines from the mixing chamber to the gas cell of an FTIR spectrometer (Nicolet 380, Thermo Fisher). When the reactor temperature reached 850 °C, at which point the desulfurization efficiency of limestone is the greatest, SO_2 gas diluted at 1100 mL/Nm^3 began to flow through the reactor in place of the Ar gas while maintaining the temperature and flow rate constant.

Transient variation of SO_2 concentration was monitored upstream and downstream in the reactor with the FTIR spectrometer. As expected, a preliminary test revealed that, with time, the ash samples as well as the limestone are gradually degraded in desulfurization capability so that the SO_2

https://dx.doi.org/10.1021/acsomega.1c00177
ACS Omega 2021, 6, 5962−5971

concentration at the exit of reactor (C_O in mL/Nm^3) rose steadily. At the moment that the SO_2 concentration became equal to the inlet concentration (C_i in mL/Nm^3), the ash sample was thought to be fully sulfated and the experiment was stopped, with the time recorded as t_T.

From the temporal variation of the C_O for a specific sample, a saturated adsorption capacity (SAC) of the sample was assessed by integrating the captured amount of SO_2 over time and normalizing the integral by the sample mass (W) as:

$$\mathrm{SAC} = \frac{Q}{W}\int_0^{t_T}(C_i - C_o)dt = \frac{C_i Q}{W}\int_0^{t_T}\left(1 - \frac{C_o}{C_i}\right)dt \quad (11)$$

where Q is the flow rate of the reactant SO_2 gas (L/min).[22,23] Note that the SAC is now expressed in units of mg·SO_2/g·sample, representing the maximum mass of SO_2 possibly removed by a gram of the ash.

3.3. Acquisition of Big Data for Desulfurization in a Large-Scale CFBC Boiler and PC Boiler. We performed statistical analysis on a complete set of field data from two 500 MW PC boilers (Hadong Thermal Power Plant Units #1 and #7) currently operating in Korea. To our knowledge, this is the first approach in the history of coal research. The field data include SO_2 concentration of flue gas measured in situ at the FGD inlet, sulfur contents (wt %) of coals, and ash compositions as well as other properties of the coals consumed for 1 year from July 2016 to July 2017. Note that the analysis of the coals has been repeated on a daily basis, producing a large size of 1300 data sets. Here, the SO_2 concentration was measured by an in situ gas analyzer (GM31, Sick).

Unlike the foregoing PC boiler, a similar data set has never been obtained from any domestic large-scale CFBC boilers. In fact, limestone and coal ashes undergo simultaneous reactions of their calcination and desulfurization, coexisting inside the furnace of CFBC boilers. This precludes a pure assessment of a fuel-born desulfurization effect independently of the limestone's contribution. Instead, we obtained a short-term test result (June 13−16, 2018) of a new 1000 MW CFBC boiler that had been constructed at Samcheok Thermal Power Plant in Korea and attempted to identify the significance of the inherent desulfurization of coal ash.

4. RESULTS AND DISCUSSION

4.1. Ash Contents vs Saturated Adsorption Capacity. Referring to Table 1, the 11 coals show large differences in their sulfur and ash contents as well as their composition. Most of the coal ashes are mainly composed of silica and alumina and are found to be porous like zeolite through quenching following high-temperature combustion. Note that some particular coal ashes contain high levels of alkali and alkali earth metals as well as iron oxide, all of which are known to play a role as desulfurization agents.[24,25]

Figure 2 shows the temporal variations of the ratio C_O/C_i of the 11 ash samples as well as the limestone sample, denoting a typical S-shape graph known as a breakthrough curve. The ratio increases quickly starting from zero and then gradually levels off around 1.0, representing the complete sulfation (or saturation of adsorption reaction) of the ash. The time to reach the ratio of unity (recorded as t_T) is quite different from sample to sample. The ratio of unity is highlighted with a dotted horizontal line for reference. It is notable that as the time t_T gets longer, an integrated area between the breakthrough curve and the unity ratio line increases proportionally, which indicates that the sample has a higher sulfur-capture capacity.

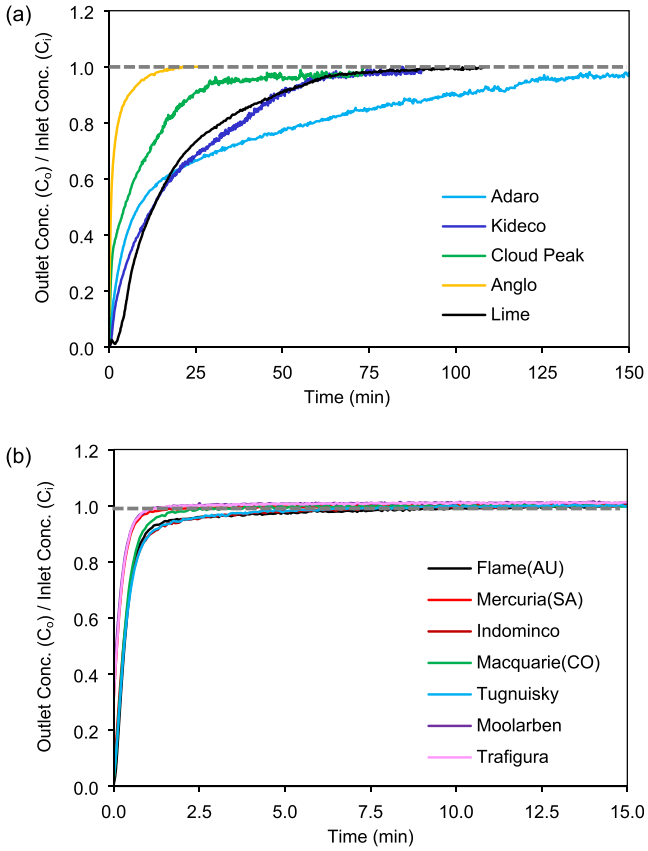

Figure 2. Breakthrough curves of 11 representative coal ash samples from lab-scale fixed bed experiments: (a) Group A and (b) Group B samples.

As such, the whole ash samples were compared in terms of the integrated areas and divided into two groups. In Figure 2a, the four ash samples from the coals of Adaro, Kideco, Anglo, and Cloud Peak, together with limestone, are classified into Group A, denoting high saturated adsorption capacities (SACs). Note that the sulfation reactions continue for 21−150 min. In contrast, Figure 2b shows that the other seven samples belonging to Group B are very rapidly saturated within 1−6 min, resulting in negligible SACs.

For a quantitative comparison between the groups, eq 11 was applied to the breakthrough curves in Figures 2a,b for calculating the SAC data per sample. Table 2 lists the SAC data of all the samples in the fifth column named "saturated", whereas the CaO and TA contents of the ash samples are shown in the first and second columns, respectively. Moreover, the third and fourth columns of Table 2 show the (theoretical) maximum capture of SO_2 per unit mass of each ash sample, particularly by CaO and TA, respectively. Note that the term "theoretical" implies the ideal case that either CaO or TA is 100% used for SO_2 capture (R' = Ca/S = 1.0 in eq 6; R'' = TA/S = 1.0 in eq. 7). Here, a ratio of the SAC to the theoretical adsorption in Table 2 may be used as a measure of maximum utilization (%) of CaO and TA in each sample and listed in the seventh and eighth columns of the table, respectively.

In Table 2, the SACs in Group A are experimentally observed in the order of Adaro > Kideco > Limestone > Cloud Peak > Anglo. This order is almost identical to the order of CaO (or

https://dx.doi.org/10.1021/acsomega.1c00177
ACS Omega 2021, 6, 5962−5971

TA) content from high to low or the theoretical adsorption of the samples in Table 2. In Group A, Adaro and Kideco ashes with high-level alkali and Fe_2O_3 components in addition to CaO show high SACs up to 130 and 91% of their theoretical (maximum) adsorptions by CaO, respectively. In contrast, the SACs of Cloud Peak and Anglo remain as low as 41 and 16% of the theoretical values, respectively. Moreover, the Group B samples that have relatively low CaO or TA contents mostly show low SACs (≤5 mg·SO_2/g·ash), corresponding to 5% or less utilization of the component, so that no inherent desulfurization effect of the ashes is expected.

It is notable that the limestone that has the highest content of CaO among the samples was not the most efficient but ranked third in Group A. In fact, the utilization of the current limestone was as low as 21%, which is much lower than the first- and second-ranked coal ash (Adaro and Kideco). One possible explanation may have to do with the difference in size between the limestone and coal ashes: 500−600 μm of the limestone vs 10−60 μm of the coal ash. Since the $CaSO_4$ layer forming on the surface of limestone during the sulfation acts as a diffusion barrier, its adverse effect on the progress of sulfation reaction might be aggravated for the 10-times larger limestone particles, resulting in the more-than-expected lowering of the utilization of the limestone. From a preliminary study, on the other hand, BET specific surface areas of three coal ash samples (Adaro, Indominco, and Moolarben) and limestone sample were found to be 1.1−5.9 and 0.15−1.56 m^2/g, respectively, both of which are too small to anticipate any discernable influence on SACs.

Figures 3a,b shows the SAC variations of the entire samples with the CaO and TA contents, respectively. Overall, the SACs are more likely correlated with TA contents compared with CaO alone (compare the R^2 scores in Figure 3a,b) In fact, the utilization based on the TA in Group A is less scattered in a range of 11−54% (compared with 16−130% of CaO; refer to Table 2). When narrowing the scope into Group A, the trend of increasing SACs with CaO/TA contents becomes more obvious in Figure 3b. Also note that the utilization of Adaro coal ash based on CaO content was 130%, which cannot be achieved, suggesting that other alkaline species must be involved in the reaction and their contribution is not negligible but at least more than 30%. These observations are apparently consistent with the claim that SO_2 capture is caused by the whole TA components, not solely by CaO.[9,10] Also note that the desulfurization function of coal ash seems to be activated in proportion to both contents but only when CaO content >0.1 mol/100 g·ash or TA content >0.2 mol/100 g·ash. The ash samples meeting this condition are mostly in Group A. These intriguing findings explain why the TA has been taken as the catalytic ash species in this study.

4.2. Desulfurization Effect of Fuel-Born Active Species in a CFBC Boiler. This section is devoted to the verification of the desulfurization effect of TA species in coal ash, particularly in the CFBC boiler. Two different coals, Kideco and Bayan, are both sub-bituminous coals that have been used for recent combustion testing of a CFBC boiler, and their sulfur and ash contents are summarized in Table 3. In Table 4, SO_2 emission data are listed with respect to coal and limestone feed rates. For reference, the inherent or total ratio of Ca/S and TA/S for each ash of the coals is included in the table. Also note that the two tables present two data sets for Kideco and Bayan, which represent that both of the coals have been tested for two different units of CFBC boiler (#1-A and #1-B units as seen in Table 4).

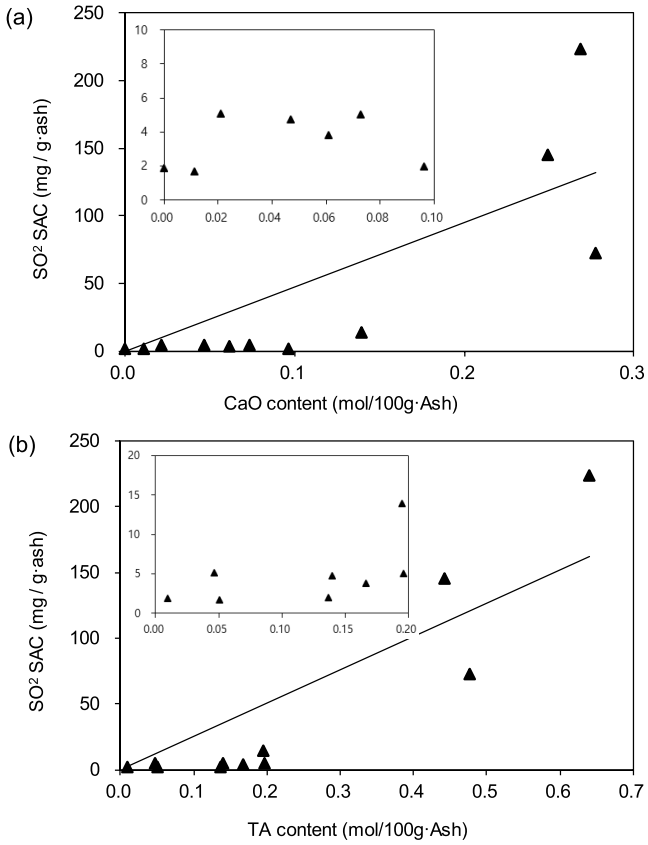

Figure 3. Relations of saturated adsorption capacity (SAC, mg·SO_2/g ash) of the samples against (a) CaO content (mol) contained in 100 g ash samples and (b) TA content (mol) contained in 100 g ash samples; insets of (a) and (b) magnify the portions of lower CaO and TA content, respectively.

Kideco and Bayan coals, which meet the design-coal standard of the boiler, have high inherent Ca/S ratios of 2.0−2.7 and (CaO equivalent) TA/S ratios of 3.5−3.9. The boiler was designed to operate with a Ca/S ratio of 3.4 to meet the SO_2 emission standard of 80 mL/Nm^3 (atmospheric emission allowance for coal-fired power plant boilers in Korea). This means that the two coals already have a considerable amount of fuel-born catalysts, suggesting that only a small addition of extra limestone would be sufficient to meet the emission standard. In reality, the SO_2 concentration was as low as 0.16−2.88 mL/Nm^3, revealing ∼97% desulfurization efficiency just by the addition of limestone at 0.8−1.2 tons/h. which correspond to a 0.6 Ca/S ratio. Upon the limestone addition, the total Ca/S ratio including the fuel-born Ca species is 2.6−3.3 lower than the design ratio of Ca/S, whereas the total TA/S ratio reaches 4.1−4.5 beyond the design ratio of TA/S. Consequently, the excellent desulfurization effect was more likely caused by the TA species in ash and not solely by Ca oxides.

Based on the desulfurization efficiency and TA contents, the utilization of fuel-born TA in the real-scale CFBC boiler is calculated to be 22−24%, which is in proximity to the SAC in between Adaro (with the highest TA content) and limestone from the fixed bed experiment (see Table 2 and Figure 3b). Since the SAC represents the cumulative SO_2 capture by coal ash until being fully saturated, the proximity of the SACs to the results of the CFBC boiler that allows a long desulfurization time by circulation is not surprising.

https://dx.doi.org/10.1021/acsomega.1c00177
ACS Omega 2021, 6, 5962−5971

Table 3. Sulfur and Ash Contents of Coals[a] and Their Ash Compositional Analysis Data

			ash ingredients (%, DB)								
coal name (country[b])	S (%, ARB)	ash (%, ADB)	SiO_2	Al_2O_3	Fe_2O_3	CaO	MgO	Na_2O	K_2O	SO_3	etc
Kideco (IDN)	0.18	5.15	24.9	6.97	30.60	20.50	10.20	0.00	0.96	4.66	1.08
Bayan (IDN)	0.15	4.52	32.60	16.70	11.50	25.50	7.08	0.53	1.14	3.18	1.25
Kideco (IDN)	0.18	4.87	29.40	8.52	29.20	17.30	8.41	0.23	1.12	4.59	1.06
Bayan (IDN)	0.16	4.53	32.30	16.50	12.40	25.40	6.62	0.64	1.14	3.23	1.36

Note: ARB, as-received basis; ADB, air-dried basis; and DB, dry basis. [a]Coals are prepared to be ∼1 mm in diameter for the preliminary combustion test of the Samcheok Thermal Power Plant boiler. [b]Country name was denoted in accordance with ISO 3166 three-letter country codes.

Table 4. Preliminary Combustion Test (June 13−16, 2018) Results of the Samcheok Thermal Power Plant Boiler (#1-a, #1-B),[a] Korea

		fuel-born sulfur & alkali contents (mol/ton·coal)			inherent molar ratio (mol/mol)			molar ratio (including limestone)			
coal name	coal feed rate (ton/h)	S	Ca	TA	Ca/S	TA/S	limestone feed rate (ton/h)	Ca/S	TA/S	SO_2 emission (mL/Nm^3 at 6% O_2)	test boiler
Kideco	270	85.2	188.3	323.8	2.2	3.8	1.0	2.84	4.4	0.16	#1-A
Bayan	287	76.2	205.5	294.3	2.7	3.9	1.0	2.62	4.1	0.16	#1-A
Kideco	260	85.8	174.0	300.5	2.0	3.5	0.8	3.32	4.5	2.88	#1-B
Bayan	279	81.9	205.2	289.7	2.5	3.5	1.2	3.32	4.4	1.78	#1-B

[a]A 1000 MW circulating fluidized bed combustion boiler consisting of two 500 MW units.

4.3. Desulfurization of Fuel-Born Active Species in a PC Boiler. Unlike CFBC boilers, the residence time of coal/ash particles is limited to a few seconds in a furnace of PC boiler and a few minutes in total before reaching an FGD unit. Such a short residence time suggests that coal ash's utilization for desulfurization is unacceptably low[26] when compared with the results of the CFBC or SAC from Table 2. Thus, it is important to measure performance degradation of fuel-born catalysts at an early stage of desulfurization that is kinetically limited. With that, the breakthrough curves in Figure 2a,b are limited to the initial 2 min portions based on a rough estimation of the residence time and are shown in Figure 4a,b, respectively.

Figure 4a shows that the top three samples in Group A (Adaro, Kideco, and Limestone) were hardly saturated in 2 min, maintaining their initial (fresh) state, whereas the samples in Group B were already fully saturated in 2 min (Figure 4b). To address the characteristics in a quantitative manner, we defined and estimated a real adsorption capacity of the samples up to 2 min (integral above each curve) by replacing the integral time t_T with 2 min in eq 11. For comparison, the 2 min adsorption capacity data of all the samples are listed in the last column of Table 2 (identified as "2 min cut"). It is noted from Table 2 that the 2 min adsorption capacity of the Group A samples reaches 6−15% of their SAC and only 2−5% of the theoretical adsorption capacity by TA as well.

We now have three indicators to assess the catalytic performance of ash or TA species: the theoretical adsorption capacity, the saturation adsorption capacity, and the 2 min adsorption capacity. The first two capacities represent a sort of intrinsic capability of ash sample for SO_2 capture given a sufficient time, as in CFBC boilers, while the last 2 min capacity presents a realistic SO_2-capture effect of fly ash particularly in PC boilers. In Figure 5, the ashes seem to be activated when TA contents exceed the threshold of 0.2 mol/100 g·ash, positioning their SACs between the theoretical capacity and the 2 min capacity. On the other hand, the 2 min adsorption data are almost negligible regardless of TA contents, suggesting that the intrinsic desulfurization effect of ashes is not expected in PC boilers.[12,19−21]

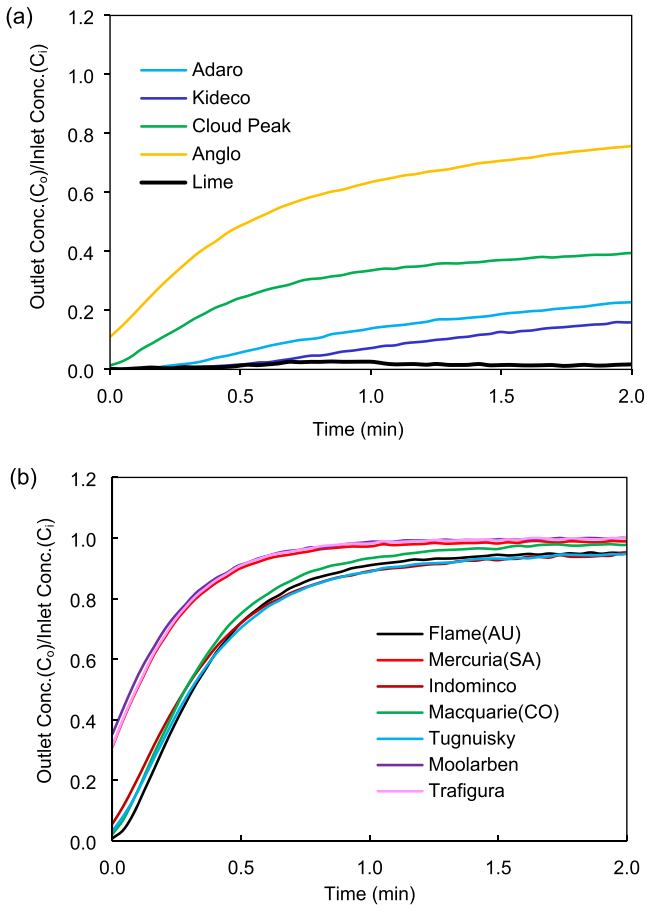

Figure 4. Early stage desulfurization characteristics of (a) Group A and (b) Group B samples during the initial 2 min with emphasis on different transient saturation behaviors of desulfurization of the groups.

https://dx.doi.org/10.1021/acsomega.1c00177
ACS Omega 2021, 6, 5962−5971

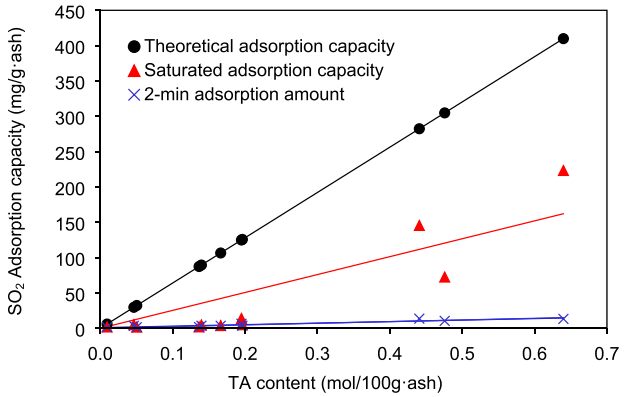

Figure 5. Comparison between the theoretical adsorption capacity (mg·SO_2/g ash), the saturated adsorption capacity (SAC, mg·SO_2/g ash), and the 2 min adsorption amount (mg·SO_2/g ash) of representative samples with different TA contents (mol/100 g ash).

The next step is to prove this speculation with the big data from the 500 MW PC boiler. Figure 6a presents a scatter plot of fuel-born SO_2 concentrations calculated by eq 1 versus TA contents of the corresponding coals in comparison with the actual SO_2 concentration data measured at the FGD inlet. As a result, the measured concentrations of SO_2 appear to be about 200 mL/Nm^3 lower on average than the calculated theoretical concentrations in the entire range of TA contents. It is notable

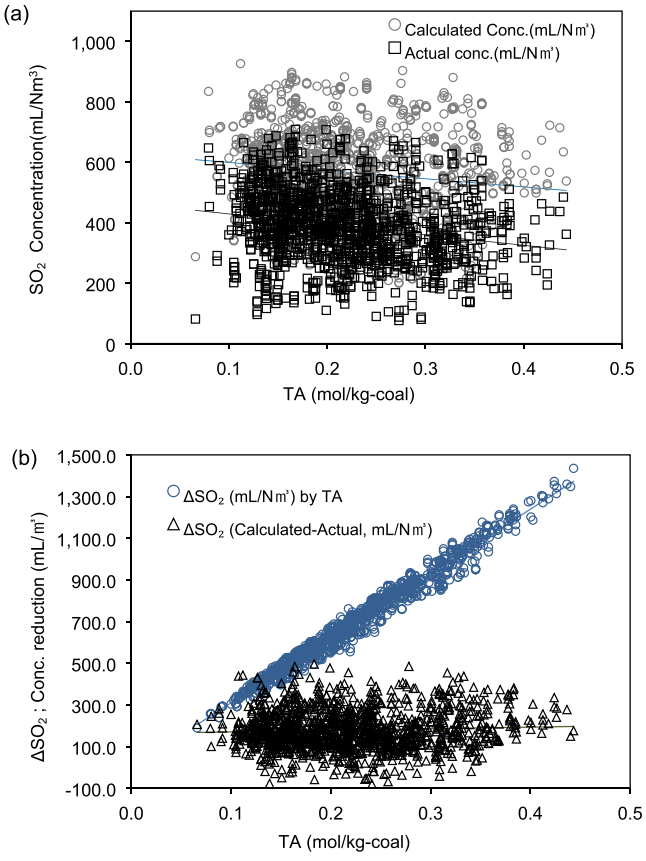

Figure 6. In-furnace desulfurization effect of TA components of the coal blends in the PC boiler, relating the calculated and actual (a) SO_2 concentrations (mL/Nm^3) and (b) SO_2 concentration reductions (ΔSO_2, mL/Nm^3) at the FGD inlet to effective TA contents (mol/kg coal) of the coal blends in the PC boiler.

that both of the concentration data are too scattered to address a certain trend. Because coal containing sulfur is the only source of SO_2 emission in PC boilers, the scattered pattern of theoretical concentration against TA content reveals that coal sulfur contents vary greatly on a daily basis irrespective of the TA content of the coal. Perhaps, this is part of the reason for concealing the fuel-born desulfurization effect in PC boilers.

To reveal the catalytic effect of TA species, we first calculated the difference ($\Delta SO_{2,actual}$) between the theoretical and the actual concentrations of SO_2, which might be regarded as an actual SO_2-reduction effect by TA, and also calculated its potential maximum reduction of SO_2 ($\Delta SO_{2,max}$) based upon 100% utilization of TA for reference. Figure 6b compares the $\Delta SO_{2,actual}$ data (denoted by a triangle) with the $\Delta SO_{2,max}$ (denoted by a circle). Note that the actual SO_2-reduction effect, though initially expected to increase with increasing TA content, appears to be very limited in the whole range of TA content and seemingly independent of the TA content. This is very likely associated with the kinetic limitation of desulfurization, which was the ″2 min cut″ shown in Figure 5 and Table 2. Thus, it can be concluded that the TA contents are not a significant factor in PC boilers.

In parallel with the sulfation reaction of eq 2, the SO_2 concentration in flue gas may be reduced via surface adsorption or vapor condensation.[1,2,10] In addition, gaseous SO_2 may react with residual oxygen and water vapor to form condensable species such as SO_3 and H_2SO_4 and can then be removed from the flue gas by vapor condensation toward the tube wall or existing ash particles. To test this scenario, the foregoing theoretical and actual SO_2 concentrations are plotted against the sulfur contents of the corresponding coals in Figure 7a. In contrast to Figure 6, the actual concentration data of SO_2 are linearly correlated with the sulfur contents of coals but always positioned lower than the theoretical values. Of greater interest, the difference between the theoretical and the actual concentrations, representing the actual reduction of SO_2 (refer to $\Delta SO_{2,actual}$ in Figure 6b), tends to increase with the sulfur content. The trend of $\Delta SO_{2,actual}$ becomes more prominent in Figure 7b, where the concentration difference obviously increases with the sulfur content. The trend was further analyzed with a linear regression, resulting in the following equation:

$$\Delta SO_2\ (\mathrm{mL/Nm^3}) = A \times S\ (\mathrm{wt\%}) + B$$
$$; A = 373.9 \pm 28.1; B = -39.4 \pm 16.9 \quad (12)$$

The linearity of the equation is attributed to the nature of vapor condensation, as follows. While the flue gas gradually cools down from 1400 °C in the furnace to 90−110 °C at the FGD inlet, the condensable acidic gases reach a high level of super-saturation that activates vapor condensation on the exhaust tube wall as well as ash particles and eventually results in a reduction of SO_2 in the flue gas.[27−30] Here, the degree of super-saturation linearly depends on the concentrations of condensable gases that increase in response to the sulfur contents of coals, which in turn boost the condensation of those gases from the flue gas in the case of high sulfur contents.

Meanwhile, there remains one last reliability issue of eq 12 arising from the data scatteredness in Figure 7b. We additionally performed the statistical analysis based on p value to verify the existence of a causal relationship between two variables (ΔSO_2 vs S content).[8] Here, the p value is a way to evaluate the resulting relationship through the hypothesis test: null hypothesis H_0 vs alternative hypothesis H_1. As a result of linear regression, the p

https://dx.doi.org/10.1021/acsomega.1c00177
ACS Omega 2021, 6, 5962−5971

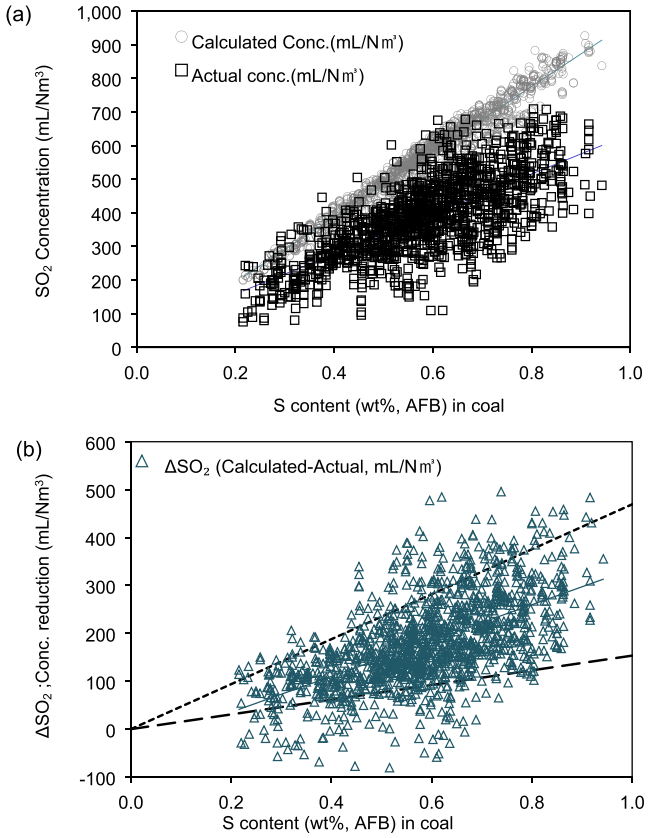

Figure 7. Effect of sulfur contents of coal blends on SO_2 emissions, relating (a) SO_2 concentration (mL/Nm^3) and (b) SO_2 concentration reduction (ΔSO_2, mL/Nm^3) at FGD inlet to effective sulfur contents (wt %, AFB) of coal blends in the PC boiler.

values for the slope and *y* intercept of eq 12 are c.o. 1.5×10^{-125} and 3.7×10^{-6}, respectively. Since both *p* values $\ll 0.05$ (in 95% confidence interval), the null hypothesis is rejected, which means that the S content is a significant factor that explains the ΔSO_2 behavior, and the resulting eq 12 is statistically meaningful.

The coefficient of determination (R^2) in eq 12 is 0.35, which accounts for about 35% of the data set (ΔSO_2 vs S content). It may seem difficult to predict the ΔSO_2 perfectly by this regression alone. As aforementioned, it is not surprising because each data point represents daily property of blended coals that should be highly scattered in nature. To provide an alternative guideline, we determined two straight lines (see the two dotted lines in Figure 7). The upper dotted line represents the upper estimation of ΔSO_2 involving 90% of the data, while the lower dotted line indicates the lower estimation of ΔSO_2 involving 90% of the data. The result shows that the upper line is expressed by $\Delta SO_2 = 469.3 \times S$, while the lower line is $\Delta SO_2 = 153.4 \times S$. Clearly, the lower line is more significant because it can be used to indicate the lowest (but guaranteed) amount of ΔSO_2. Based on this lower estimation, boiler engineers might be able to make a conservative decision of the maximum (required) feed rate of limestone for meeting the emission limit as follows. One may want to predict the concentration of SO_2 at their FGD inlet ($C_{SO2,FGD}$) under the current circumstance. For this purpose, eq 12 is rearranged with respect to $C_{SO2,FGD}$, as shown in eq 13, recalling the definitions of *S*, G_w, and ΔSO_2 in eqs 1 and 12.

$$C_{SO2,FGD}\ (\mathrm{mL/Nm^3}) = \frac{0.7 \times S}{G_w} \times 10^6 - \Delta SO_2 \quad (13)$$

Since the acid dew point determining the condensation rate is known to rely not only on the sulfur contents but also on the cooling rate, fuel supply rate, and boiler designs, one may notice that eqs 12 and 13 are valid only for the 500 MW PC boiler we tested. In other words, applying eq 13 for other types of furnace beyond the PC boiler is questionable. However, it should be noted that our big-data-based approach for the prediction of apparent SO_2 concentration prior to boiler operation, such as in eqs 12 and 13, can be considered a practical method for economic and eco-friendly operation of PC boilers once a specific boiler has been tested likewise.

5. CONCLUSIONS

In this study, we performed a series of temperature-controlled fixed bed (lab scale) experiments for 11 individual (but representative) coal samples. As a result, the desulfurization appeared to be driven by the total alkali (TA) contents of the ashes rather than the calcium species alone, leading to a classification of the samples into two groups in terms of saturated adsorption capacity (SAC). The group of samples with a high SAC was further proven to be effective for fuel-born desulfurization, indicating the high utilization of the TA component. This lab-scale result was supported by a preliminary field test of a 1000 MW CFBC boiler in Korea. For comparison, we also established a complete database by recording the thermochemical properties and emission characteristics of coal blends for 1 year in a 500 MW PC boiler in Korea. Interestingly, we found that the TA components did not impart any discernable effect on SO_2 concentration measured at the FGD inlet of the PC boiler, which was in contrast to the CFBC boiler. Instead, the SO_2 concentration was correlated with the sulfur content of the coal blends, resulting in a simple equation that can be practically used for a priori prediction of SO_2 concentration in a PC boiler. The result was attributed to the kinetic limitation of fuel-born desulfurization reaction in the PC boiler and seemingly associated with the initial 2 min behaviors of the ash samples from the fixed bed experiment. Our last conclusive remark would be related to a future study plan with emphasis on the possibility that not all AAEM species might play an equal role in dry desulfurization. We are planning to monitor the SO_2 emissions from a large-scale CFBC boiler likewise in parallel with impact assessment of each AAEM component.

AUTHOR INFORMATION

Corresponding Author

Donggeun Lee − *School of Mechanical Engineering, Pusan National University, Busan 46241, South Korea;* orcid.org/0000-0001-7256-1956; Phone: 82-51-510-2365; Email: donglee@pusan.ac.kr; Fax: 82-51-512-5236

Authors

Dong-Yeop Kim − *School of Mechanical Engineering, Pusan National University, Busan 46241, South Korea; Combustion Technology Center, Hadong Thermal Power Site Division, Korea Southern Power Co., Busan 52353, South Korea*

In-Duck Cheong − *School of Mechanical Engineering, Pusan National University, Busan 46241, South Korea*

Jeonggeon Kim − *School of Mechanical Engineering, Pusan National University, Busan 46241, South Korea*

Complete contact information is available at:

https://dx.doi.org/10.1021/acsomega.1c00177
ACS Omega 2021, 6, 5962−5971

https://pubs.acs.org/10.1021/acsomega.1c00177

Notes

The authors declare no competing financial interest.

■ ACKNOWLEDGMENTS

This work was supported by the National Research Foundation of Korea for the research project of NRF-2020R1A2C2011634.

■ REFERENCES

(1) Belo, L. P.; Spörl, R.; Shah, K. V.; Elliott, L. K.; Stanger, R. J.; Maier, J.; Wall, T. F. Sulfur capture by fly ash in air and oxy-fuel pulverized fuel combustion. *Energy Fuels* **2014**, *28*, 5472−5479.
(2) Srivastava, R. K.; Miller, C. A.; Erickson, C.; Jambhekar, R. Emissions of sulfur trioxide from coal-fired power plants. *J. Air Waste Manage. Assoc.* **2004**, *54*, 750−762.
(3) Bartels, M.; Lin, W.; Nijenhuis, J.; Kapteijn, F.; van Ommen, J. R. Agglomeration in fluidized beds at high temperatures : Mechanisms, detection and prevention. *Prog. Energy Combust. Sci.* **2008**, *34*, 633−666.
(4) Boskovic, S.; Reddy, B. V.; Basu, P. Effect of operating parameters on sulphur capture in a pressurized circulating fluidized bed combustor. *Int. J. Energy Res.* **2002**, *26*, 173−183.
(5) Basu, P. *Circulating Fluidized Bed Boilers*; Design, Operation and Maintenance. Springer: 2013, 128−143.
(6) Leckner, B. Optimization of emissions from fluidized bed boilers. *Int. J. Energy Res.* **1992**, *16*, 351−363.
(7) Zygarlicke, C. J.; Stomberg, A. L.; Folkedahl, B. C.; Strege, J. R. Alkali influences on sulfur capture for North Dakota lignite combustion. *Fuel Process. Technol.* **2006**, *87*, 855−861.
(8) Sotiropoulos, D.; Georgakopoulos, A.; Kolovos, N. Impact of free calcium oxide content of fly ash on dust and sulfur dioxide emissions in a lignite-fired power plant. *J. Air Waste Manage. Assoc.* **2005**, *55*, 1042−1049.
(9) Davis, W. T.; Fiedler, M. A. The retention of sulfur in fly ash from coal-fired boilers. *J. Air Waste Manage. Assoc.* **1982**, *32*, 395−397.
(10) Spörl, R.; Walker, J.; Belo, L.; Shah, K.; Stanger, R.; Maier, J.; Wall, T.; Scheffknecht, G. SO_3 emissions and removal by ash in coal-fired oxy-fuel combustion. *Energy Fuels* **2014**, *28*, 5296−5306.
(11) Belo, L. P.; Elliott, L. K.; Stanger, R. J.; Spörl, R.; Shah, K. V.; Maier, J.; Wall, T. F. High-temperature conversion of SO_2 to SO_3 : Homogeneous experiments and catalytic effect of fly ash from air and oxy-fuel firing. *Energy Fuels* **2014**, *28*, 7243−7251.
(12) Cheng, J.; Zhou, J.; Liu, J.; Zhou, Z.; Huang, Z.; Cao, X.; Zhao, X.; Cen, K. Sulfur removal at high temperature during coal combustion in furnaces: a review. *Prog. Energy Combust. Sci.* **2003**, *29*, 381−405.
(13) Mathieu, Y.; Tzanis, L.; Soulard, M.; Patarin, J.; Vierling, M.; Molière, M. Adsorption of SOx by oxide materials: a review. *Fuel Process. Technol.* **2013**, *114*, 81−100.
(14) Wang, L.; Li, S.; Eddings, E. G. Fundamental study of indirect vs direct sulfation under fluidized bed conditions. *Ind. Eng. Chem. Res.* **2015**, *54*, 3548−3555.
(15) Li, W.; Li, S.; Xu, M.; Wang, X. Study on the limestone sulfation behavior under oxy-fuel circulating fluidized bed combustion condition. *J. Energy Inst.* **2018**, *91*, 358−368.
(16) Poullikkas, A. Review of design, operating, and financial considerations in flue gas desulfurization systems. *Energy Technol. Policy* **2015**, *2*, 92−103.
(17) Anthony, E. J.; Granatstein, D. L. Sulfation phenomena in fluidized bed combustion systems. *Prog. Energy Combust. Sci.* **2001**, *27*, 215−236.
(18) Shih, S.-M.; Lai, J.-C.; Yang, C.-H. Kinetics of the reaction of dense CaO particles with SO_2. *Ind. Eng. Chem. Res.* **2011**, *50*, 12409−12420.
(19) Snow, M. J. H.; Longwell, J. P.; Sarofim, A. F. Direct sulfation of calcium carbonate. *Ind. Eng. Chem. Res.* **1988**, *27*, 268−273.
(20) Doğu, T. The importance of pore structure and diffusion in the kinetics of gas-solid non-catalytic reactions: Reaction of calcined limestone with SO_2. *Chem. Eng. J.* **1981**, *21*, 213−222.
(21) Lee, K. T.; Koon, O. W. Modified shrinking unreacted-core model for the reaction between sulfur dioxide and coal fly ash/CaO/$CaSO_4$ sorbent. *Chem. Eng. J.* **2009**, *146*, 57−62.
(22) Liu, H. N.; Zhang, H. F.; Gao, C.; Ye, X. S.; Wu, Z. J. Adsorption breakthrough curves for alkaline-earth metal ions on the resins in a fixed-bed column. *Adv. Mater. Res.* **2014**, *884-885*, 16−20.
(23) Chowdhury, Z. Z.; Hamid, S. B. A.; Zain, S. M. Evaluating design parameters for breakthrough curve analysis and kinetics of fixed bed columns for Cu(II) cations using lignocellulosic wastes. *BioResources* **2014**, *10*, 732−749.
(24) Yang, R. T.; Shen, M.-S.; Steinberg, M. Fluidized-Bed Combustion of coal with lime additives: Catalytic sulfation of lime with iron compounds and coal ash. *Environ. Sci. Technol.* **1978**, *12*, 915−918.
(25) Ahmaruzzaman, M.; Gupta, V. K. Application of coal fly ash in air quality management. *Ind. Eng. Chem. Res.* **2012**, *51*, 15299−15314.
(26) Yadav, S.; Mondal, S. S. A complete review based on various aspects of pulverized coal combustion. *Int. J. Energy Res.* **2019**, *43*, 3134−3165.
(27) Ahn, J.; Okerlund, R.; Fry, A.; Eddings, E. G. Sulfur trioxide formation during oxy-coal combustion. *Int. J. Greenhouse Gas Control* **2011**, *5*, S127−S135.
(28) Raask, E. Sulphate capture in ash and boiler deposits in relation to SO_2 emission. *Prog. Energy Combust. Sci.* **1982**, *8*, 261−276.
(29) Ock, Y.; Kim, J.; Choi, I.; Kim, D. S.; Choi, M.; Lee, D. Size-independent unipolar charging of nanoparticles at high concentrations using vapor condensation and its application for improving DMA size-selection efficiency. *J. Aerosol Sci.* **2018**, *121*, 38−53.
(30) Pyo, J.; Ock, Y.; Jeong, D.; Park, K.; Lee, D. Development of filter-free particle filtration unit utilizing condensational growth: with special emphasis on high-concentration of ultrafine particles. *Build. Environ.* **2017**, *112*, 200−208.

https://dx.doi.org/10.1021/acsomega.1c00177
ACS Omega 2021, 6, 5962−5971